THE MICROSTRUCTURE, MARTENSITIC TRANSFORMATION BEHAVIORS AND MECHANICAL PROPERTIES OF TINIHF COMPOSITE CONTAINING TIB WHISKER AND $(TI,HF)_2NI$ PARTICLE

Xiaoyang Yi[1], Xianglong Meng[2] and Wei Cai[3]

[1] School of Materials Science and Engineering, Harbin Institute of Technology, 15B909003@hit.edu.cn
[2] School of Materials Science and Engineering, Harbin Institute of Technology, xlmeng@hit.edu.cn
[3] School of Materials Science and Engineering, Harbin Institute of Technology, weicai@hit.edu.cn

Keywords: Ti-Ni-Hf composite, high temperature shape memory alloy, microstructure, martensitic transformation, mechanical properties

ABSTRACT

Ti-Ni-Hf composite containing different second phases was fabricated by hot pressed sintering process and the microstructure, martensitic transformation behaviours and mechanical properties were systematically characterized by SEM, TEM, DSC and compressive test. The results showed that the microstructure of Ti-Ni-Hf composite consisted of martensite phase (B19'), TiB whisker and $(Ti,Hf)_2Ni$ particle. The precipitation and formation of the second phase mainly occurred at the surface of original alloy powder. In addition, the Ti-Ni-Hf composite not only showed relatively higher transformation temperature (>100 ^oC), but also exhibited excellent compressive strength, which provided a novel method for designing the high temperature shape memory alloy with higher strength.

1 INTRODUCTION

Ti-Ni-Hf based shape memory alloy have been paid more attention because of the higher transformation temperatures with the critical 100 oC to 520 oC temperature range, high work output and two-way shape memory effect and so on [1-3]. However, the shape memory properties of Ti-Ni-Hf based alloy limits the extensive application due to the low matrix strength [3,4]. Up to now, the main methods such as thermo-mechanical treatment, precipitation hardening and solution strengthening as well as the combination of these methods have been adopted to enhance the matrix strength in Ti-Ni-Hf alloy [5-9]. Although the strength of the matrix is improved by the above mentioned way to some extent, the martensitic transformation temperatures are reduced significantly or even less than 100 ^oC [5-9]. Ideally, the mechanical properties can be improved and without sacrificing the martensitic transformation temperatures. It has been reported that the randomly dispersed nano-sized SiC particle and several types of second phase particles in the matrix of the Ti-Ni shape memory alloy composite not only can reinforce the matrix of the alloy, but also slightly affect the phase transformation characteristics [10].The ultimate strength of 2.54 GPa and the maximum plastic strain of 35.6% can be achieved in the in situ nanolamellar Ti_5Si_3/TiNi composite [11]. In addition, the network structure formed by the TiB whisker plays an important role in improving the mechanical properties based on the H-S theory [12,13]. Thus, the improvement of strength in the Ti-Ni-Hf alloy is expected to achieve by the combination of second phase particle/whisker and the construction of network structure in the present study.

In order to achieve the goal, the Ti-Ni-Hf composite reinforced by the second phase and the network structure is fabricated by powder metallurgy process and the microstructure, martensitic transformation behaviours and mechanical properties are investigated systematically.

2 EXPERIMENT

The spherical Ti-Ni-Hf alloy powders with the particle size of φ 45 ~ 75 μm and the TiB_2 particles with the size of about 4μm were used for original material. In order to the TiB_2 particle attach to the surface of Ti-Ni-Hf alloy powder. The mixture of Ti-Ni-Hf alloy powder and TiB_2 particle was obtained by the low-energy milling with the following parameters: rotating speed: 200 r/min, milling time: 6 h and ball-to-powder ratio = 5:1. The whole process is under Ar atmosphere. Then the mixture was sintered at 1100 ^oC for 1 h by hot-pressed sintering (HPS). The sintering process was under vacuum condition and at a pressure of 60 MPa. The details of the fabrication were illustrated in Fig. 1.

The samples for XRD, SEM, TEM, DSC and compressive test were obtained by electro-discharge cutting from the sintered Ti-Ni-Hf composite. The identification of phase was carried out using X-ray diffraction with Cu Kα radiation. Microstructural analysis was conducted by SEM and TEM. Transformation temperature and behaviours were examined by DSC tests with cooling and heating rates of 20 K/min from -100 ^oC to 200 ^oC. The mechanical properties were characterized by compressive test with the loading/unloading speed of 0.2 mm/min.

3 RESULTS AND DISCUSSION

Fig. 2 showed the XRD pattern of the Ti-Ni-Hf composite. The main peaks in the XRD pattern can be indexed as B19' martensite with the following lattice parameters: a = 0.2458 nm; b = 0.4085 nm; c = 0.4796 nm; β = 99.48^o. In addition, other minor diffraction peaks can be indexed as the mixture of orthorhombic TiB and face-centered cubic $(Ti,Hf)_2Ni$ phase using the following lattice parameters: a_{TiB} = 0.610 nm, b_{TiB} = 0.308 nm, c_{TiB} = 0.452 nm and $a_{(Ti,Hf)2Ni}$ = 1.132 nm, which indicated that the precipitation of $(Ti,Hf)_2Ni$ and the reaction of $Ti+TiB_2 \rightarrow TiB$ occurred during the hot pressed sintering process and the following cooling process.

Fig. 3 exhibited the backscattered electron images of the Ti-Ni-Hf composite. Obviously, the addition of TiB_2 particles resulted in the change in microstructure and phase constituents of the Ti-Ni-Hf composite. It can be seen from Fig. 3(a) that the microstructure was comprised of masses of network structure with the size of about 50μm, which was determined by the size of the original alloy powder. By careful observation at the high magnification and combined with the EDS results, the network structure consisted of the $(Ti,Hf)_2Ni$ particle and the TiB whisker phases. Moreover, a portion of $(Ti,Hf)_2Ni$ particle and TiB whisker phases also can be observed in the interior of the network structure. Such results were well in agreement with the results of XRD. According to the Ti-Ni-Hf ternary phase diagram, the $(Ti,Hf)_2Ni$ can formed easily at the sintering temperature of 1100 ^oC. The reaction of $Ti+TiB_2 \rightarrow TiB$ was easier to occur owing to the lower Gibbs energies of TiB.

To further identity the phase in the Ti-Ni-Hf composite, the TEM bright field observation and the corresponding electron diffraction patterns were carried out and the results were shown in Fig. 4. As reported in the Ti-Ni-Hf based alloy [14], the martensite mainly showed lath-like and spear-like, forming the typical self-accommodation configuration. In addition, the TiB whisker with about 600 nm in width was observed among the martensite. It can be confirmed by the corresponding electron diffraction patterns in Fig. 4(b) taken from the A zone in (a). Besides, the $(Ti,Hf)_2Ni$ phase with the irregular shape was found in Fig. 4(c), which can be verified by the corresponding electron diffraction patterns in Fig. 4(d).

The DSC curve of Ti-Ni-Hf composite was showed in Fig. 5. As reported in the previous study [15,16], only one endothermic and exothermic peak can be found in the heating and cooling curves respectively, which indicated that only single stage martensitic transformation (B2⇋B19') occurred during the heating and cooling process. Compared with the Ti-Ni-Hf alloy, the transformation temperatures of Ti-Ni-Hf composite was lower as a result of the dissipation and precipitation of Ti in

the matrix. Despite, the forward martensitic transformation temperature (M_s) was 152.23 ^oC, which can meet the application of high temperature fields. In addition, the dependence of martensitic transformation temperature on the thermal cycles was plotted in Fig. 5(b). Similarly, with the thermal cycles increasing, the martensitic temperature decreased significantly in the initial five cycles and then became stable in the following thermal cycles. The reverse martensitic transformation peak temperature (A_p) and forward martensitic transformation peak temperature (M_p) decreased by about 18 ^oC and 13 ^oC after 20 thermal cycles, respectively. The reduction of transformation temperature can be related to the generation of dislocations owing to the lattice mismatch between the martensite and austenite during the thermal cycling [17].

Fig. 6 showed the stress-strain curve of Ti-Ni-Hf composite. For comparison, the stress-strain curve of the casted Ti-Ni-Hf alloy also drawn in Fig. 6. Similarly, both the Ti-Ni-Hf alloy and Ti-Ni-Hf composite were characterized by the continuous yielding and high work-hardening. In addition, the Ti-Ni-Hf composite exhibited the higher compressive strength. The maximum compressive fracture strength can achieve approximately 2.4 GPa. In the Ti-Ni-Hf composite, one the one hand, both the $(Ti,Hf)_2Ni$ phase and TiB phase distributed in the matrix, which can improve the mechanical properties; on the other hand, based on the H-S theory, the microstructure of Ti-Ni-Hf composite can be regarded as the soft matrix surrounded by the hard $(Ti,Hf)_2Ni$ phase and TiB phase, the forming network structure played an important role in the improvement of the compressive strength.

4 CONCLUSIONS

The microstructure, martensitic transformation and mechanical properties of Ti-Ni-Hf composite were investigated systematically. The obtained results were as follows:

(1) The microstructure consisted of martensite phase (B19'), $(Ti,Hf)_2Ni$ phase and TiB phase. The $(Ti,Hf)_2Ni$ phase and TiB phase formed at the surface of original alloy powder. Besides, a portion of second phases also can be found in the interior of original alloy powder.

(2) The Ti-Ni-Hf composite showed the relative higher martensitic transformation temperature of Ms～152^oC.

(3) The TiNiHf composite exhibited the higher compressive strength as a consequence of the precipitation of $(Ti,Hf)_2Ni$ phase and formation of TiB phase as well as the construction of network structure.

ACKNOWLEDGEMENTS

This work was supported by the the National Natural Science Foundation of China (Nos. 51322102 and 51571073) and State Key Lab of Advanced Metals and Materials (2015-Z01).

REFERENCES

[1] Angst D R, Thoma P E, Kao M Y. The Effect of Hafnium Content on the Transformation Temperatures of Ni49Ti51-xHfx. Shape Memory Alloys. Journal de physique IV, 1995, 5(C8): C8-747-C8-752.
[2] Meng X L, Zheng Y F, Cai W, et al. Two-way shape memory effect of a TiNiHf high temperature shape memory alloy. Journal of alloys and compounds, 2004, 372(1): 180-186.
[3] Karaca H E, Acar E, Tobe H, et al. NiTiHf-based shape memory alloys. Materials Science and Technology, 2014, 30(13): 1530-1544.
[4] Meng X L, Zheng Y F, Wang Z, et al. Shape memory properties of the Ti 36 Ni 49 Hf 15 high temperature shape memory alloy. Materials Letters, 2000, 45(2): 128-132.
[5] Kockar B, Karaman I, Kim J I, et al. A method to enhance cyclic reversibility of NiTiHf high temperature shape memory alloys. Scripta Materialia, 2006, 54(12):2203-2208.

[6] Meng X L, Zheng Y F, Wang Z, et al. Effect of aging on the phase transformation and mechanical behavior of Ti 36 Ni 49 Hf 15, high temperature shape memory alloy. Scripta Materialia, 2000, 42(4):341-348.
[7] Yi X, Gao W, Meng X, et al. Martensitic transformation behaviors and mechanical properties of (Ti 36 Ni 49 Hf 15) 100-x Y x high temperature shape memory alloys. Journal of Alloys and Compounds, 2017, 705: 98-104.
[8] Dai Hsu D H, Hornbuckle B C, Valderrama B, et al. The effect of aluminum additions on the thermal, microstructural, and mechanical behavior of NiTiHf shape memory alloys. Journal of Alloys and Compounds, 2015, 638: 67-76.
[9] Kim H Y, Jinguu T, Nam T, et al. Cold workability and shape memory properties of novel Ti–Ni–Hf–Nb high-temperature shape memory alloys. Scripta Materialia, 2011, 65(9): 846-849.
[10] Jiang H J, Cao S, Ke C B, et al. Nano-sized SiC particle reinforced NiTi alloy matrix shape memory composite. Materials Letters, 2013, 100: 74-77.
[11]Jiang D, Hao S, Zhang J, et al. In situ synchrotron investigation of the deformation behavior of nanolamellar Ti_5Si_3/TiNi composite. Scripta Materialia, 2014, 78: 53-56.
[12] Huang L J, Geng L, Peng H X, et al. Effects of sintering parameters on the microstructure and tensile properties of in situ, TiBw/Ti6Al4V composites with a novel network architecture. Materials & Design, 2011, 32(6):3347–3353.
[13] Huang L J, Geng L, Li A B, et al. In situ TiBw/Ti–6Al–4V composites with novel reinforcement architecture fabricated by reaction hot pressing. Scripta Materialia, 2009, 60(11):996-999.
[14] Meng X L, Cai W, Fu Y D, et al. Martensite structure in Ti–Ni–Hf–Cu quaternary alloy ribbons containing (Ti, Hf) 2 Ni precipitates. Acta Materialia, 2010, 58(10): 3751-3763.
[15] Meng X L, Fu Y D, Cai W, et al. Microstructure and martensitic transformation behaviors of a Ti–Ni–Hf–Cu high-temperature shape memory alloy ribbon. Philosophical Magazine Letters, 2009, 89(7): 431-438.
[16] Tong Y, Chen F, Tian B, et al. Microstructure and martensitic transformation of Ti 49 Ni 51− x Hf x high temperature shape memory alloys. Materials Letters, 2009, 63(21): 1869-1871.
[17] Hsieh S F, Wu S K, Lin H C. Martensitic transformation of a Ti-rich Ti 51 Ni 47 Si 2 shape memory alloy. Journal of alloys and compounds, 2002, 335(1): 254-261.

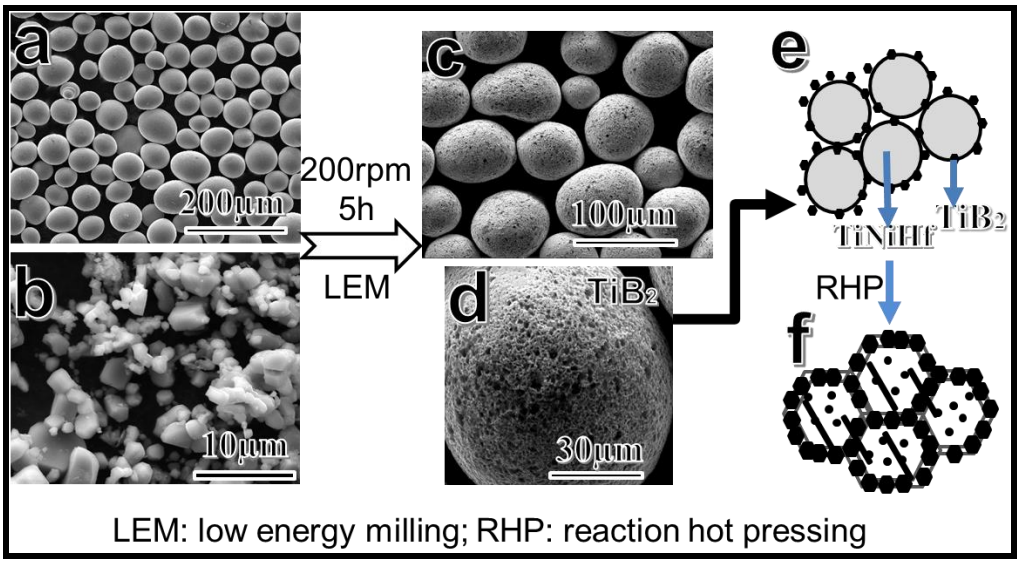

Fig. 1 Flow chart showing the processing route together with SEM micrographs of raw materials and schematic illustrations of network distribution.

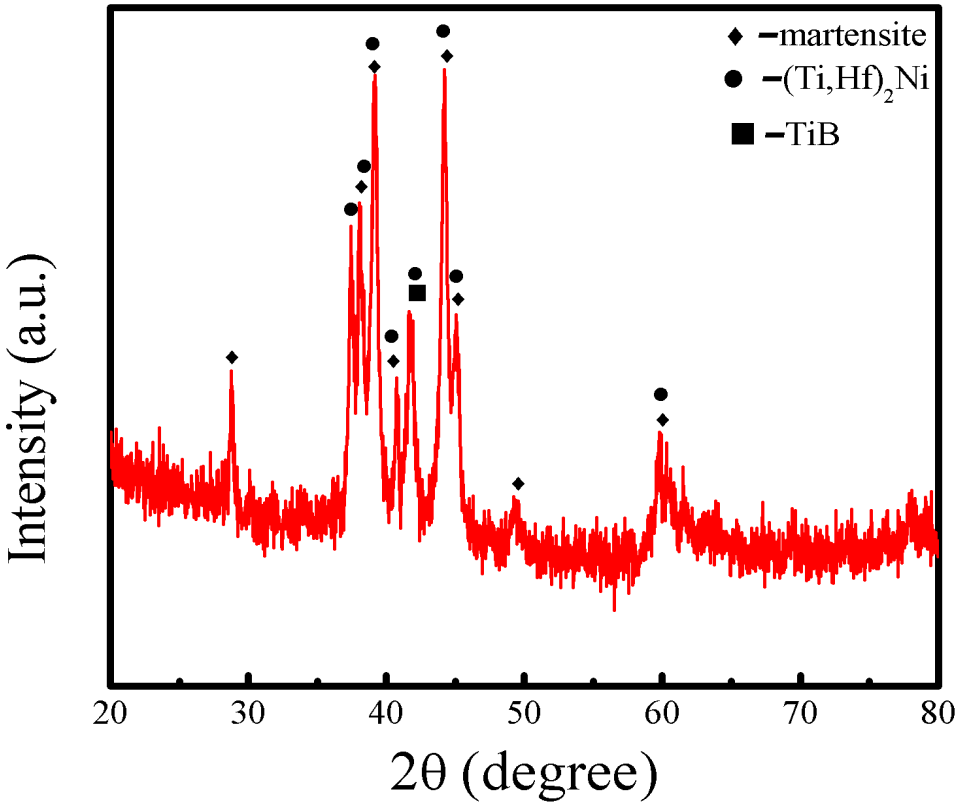

Fig. 2 The XRD patterns of the sintered Ti-Ni-Hf composite

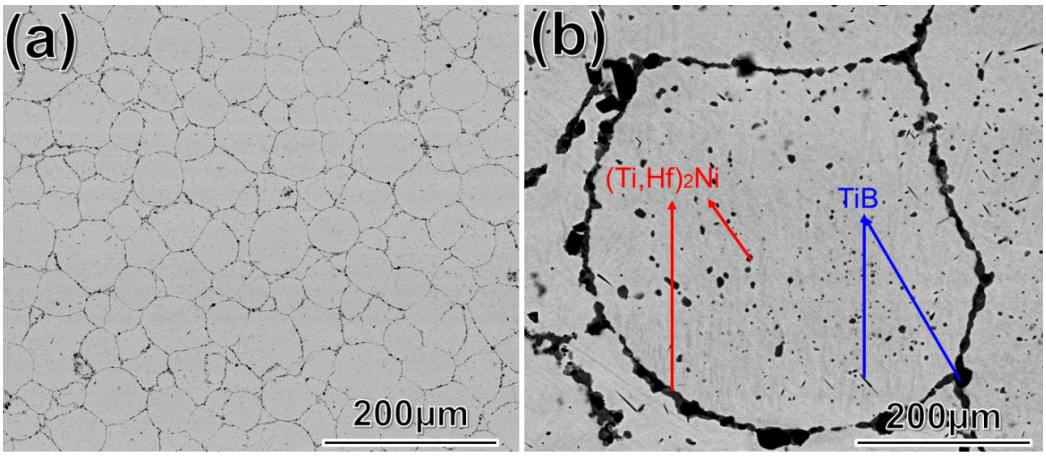

Fig. 3 The SEM micrographs of the Ti-Ni-Hf composite (a): low magnification (b): high magnification

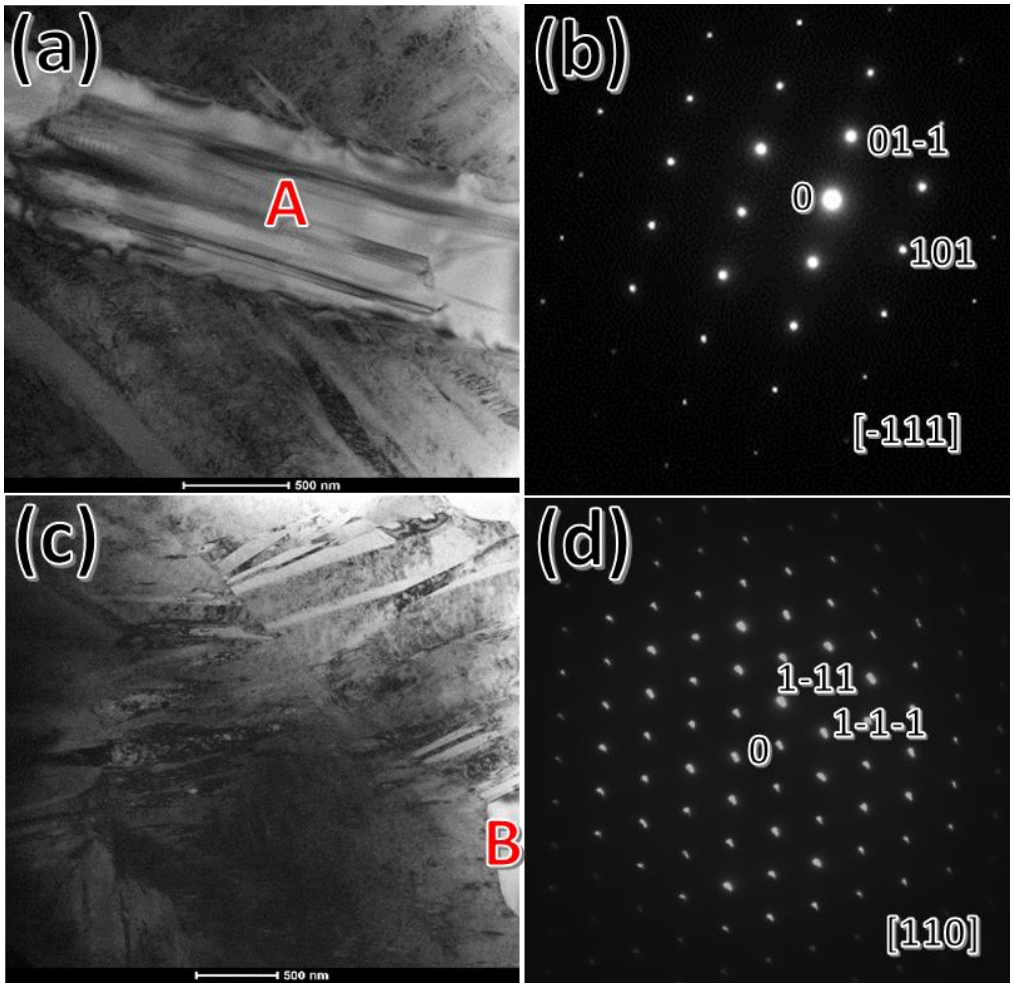

Fig. 4 The bright field images and corresponding electron diffraction patterns (a): the bright field images of the martensite and TiB phase; (b): electron diffraction pattern taken from region A in (a); (c): the bright field images of the martensite and $(Ti,Hf)_2Ni$ phase; (d): electron diffraction pattern taken from region B in (c)

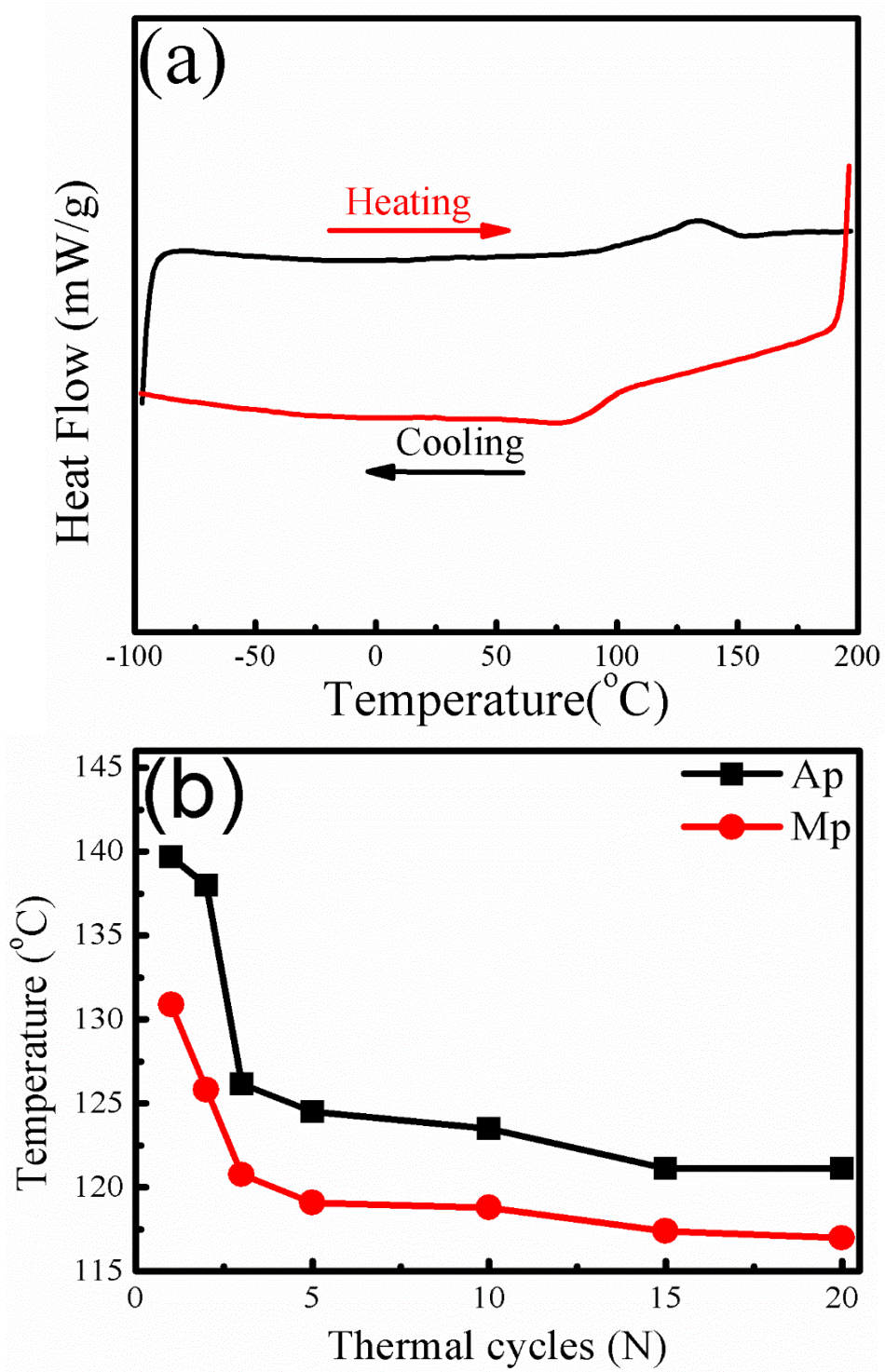

Fig. 5 The martensitic transformation behaviors of Ti-Ni-Hf composite (a): The DSC curve of the Ti-Ni-Hf composite (b): The dependence of the transformation temperatures on the thermal cycles

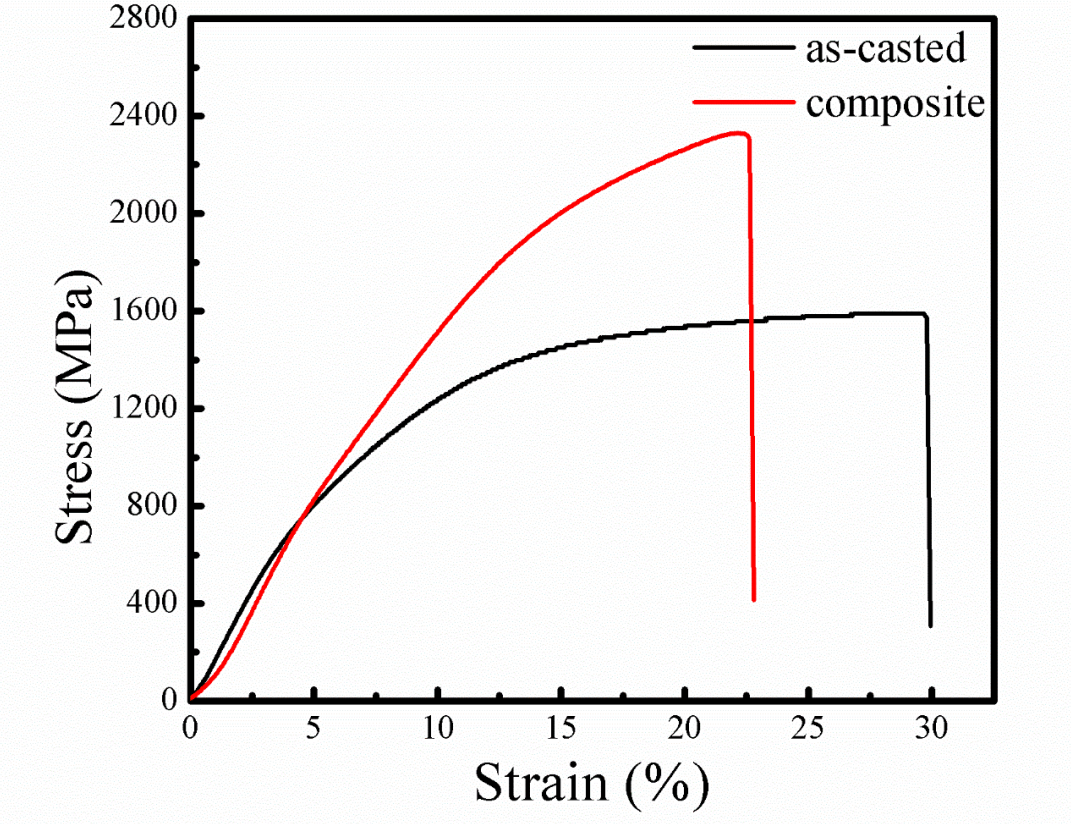

Fig. 6 the stress-strain curve of the as-casted Ti-Ni-Hf alloy and Ti-Ni-Hf composite